On the Nucleosynthesis of Nitrogen

James W. Johnson

CCSN and AGB Star Yields of Nitrogen

Core-Collapse Supernova Yields

Empirically, nitrogen-to-oxygen ratios exhibit a plateau at log(N/O) ≈ -1.5 for log(O/H) $\lesssim 8$ (see Fig. 1 of Vincenzo et al., 2016 comparing Berg et al., 2012, Izotov, Thuan & Guseva, 2012, and James et al., 2015 measurements).

What is the implied relation between the IMF integrated CCSN yields of nitrogen and oxygen?

The ratio of their yields can be related to the number densities of the two nuclei in the supernova ejecta via:

$$\frac{y_{\rm N}^{\rm CC}}{y_{\rm O}^{\rm CC}} = \frac{\mu_{\rm N} n_{\rm N}}{\mu_{\rm O} n_{\rm O}} \tag{1}$$

where μ_x is the mean molecular weight of a species x and n_x is the number of nuclei. Taking the ratio $n_{\rm N}/n_{\rm O}$ from these observed results yields:

$$\frac{y_{\rm N}^{\rm CC}}{y_{\rm O}^{\rm CC}} = \frac{\mu_{\rm N}}{\mu_{\rm O}} 10^{\log({\rm N/O})} \tag{2}$$

Though supernova ejecta may produce different isotopic ratios of N than AGB stars, potentially altering the ratio $\mu_{\rm N}/\mu_{\rm O}$, taking $\mu_{\rm N} = 14.007$ and $\mu_{\rm O} = 15.999$ from a periodic table suggests that, with the previously adopted $y_{\rm O}^{\rm CC} = 0.015$ (e.g. Weinberg, Andrews & Freudenburg, 2017; Johnson & Weinberg, 2020; Johnson et al., 2021), this suggests

$$y_{\rm N}^{\rm CC} = \frac{\mu_{\rm N}}{\mu_{\rm O}} 10^{\log({\rm N/O})} y_{\rm O}^{\rm CC} = \frac{14.007}{15.999} 10^{-1.5} (0.015) \approx 4.15 \times 10^{-4} \tag{3}$$

Can this be understood from theoretically predicted yields?

The left panel of Figure 1 presents the IMF-integrated yields $y_{\rm N}^{\rm CC}$ computing with VICE using the Limongi & Chieffi (2018), Sukhbold et al. (2016), Nomoto et al. (2013), and Woosley & Weaver (1995) CCSN yield tables, with Limongi & Chieffi (2018) being the only study which reports yields for rotating progenitors. Broadly, the non-rotating predictions are consistent with one another, and predict a significant metallicity dependence; the lowest metallicity progenitor from Woosley & Weaver (1995) predict somewhat higher yields overall, but this could have to do with this being the only yield set for which we can calculate only *gross* yields rather than *net* yields. The rotating progenitors from Limongi & Chieffi (2018), however, predict that the yield should be considerably enhanced by rotation. They interpret this as being due to the interplay between the core helium and hydrogen burning shells triggered by rotation-induced instabilities, which drives the synthesis of all products of CNO, not just ^{14}N (see their abstract). These yields predict a relatively metallicity-independent $y_{\rm N}^{\rm CC}$ of $\sim 5\times10^{-4}$, in surprisingly good agreement with the empirically derived value of 4.15×10^{-4}.

The right panel of Figure 1 presents the IMF-integrated nitrogen-to-oxygen ratios predicted by the same studies for the same combinations of metallicity and rotational velocity.

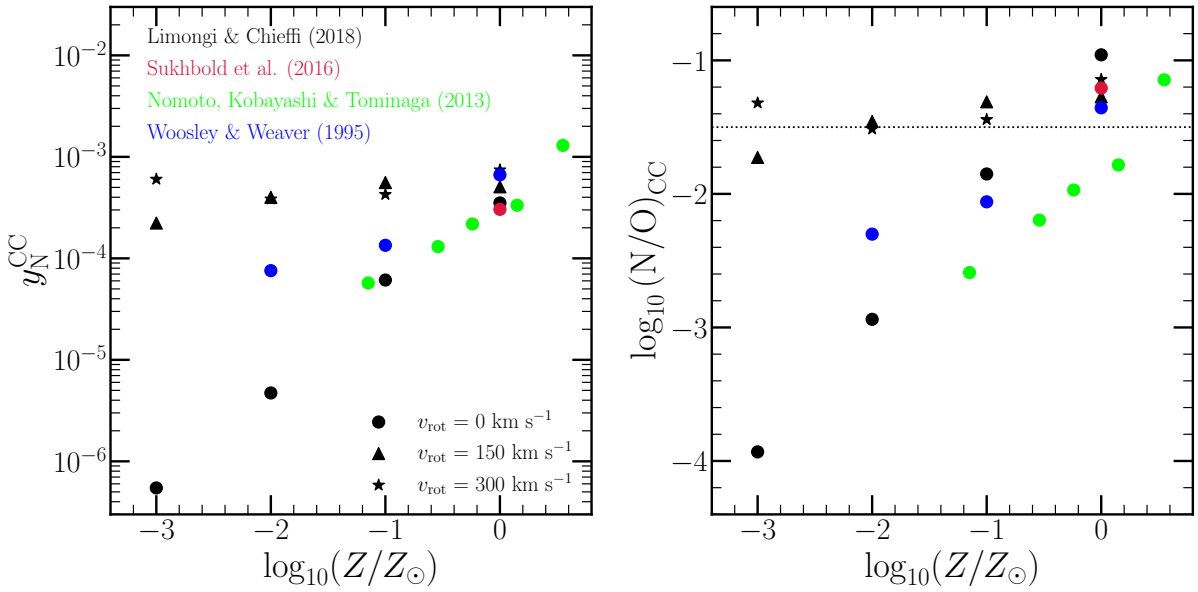

Figure 1: **Right**: IMF-integrated CCSN yields of N computed with VICE using the Limongi & Chieffi (2018) (black), Sukhbold et al. (2016) (crimson), Nomoto et al. (2013) (lime), and Woosley & Weaver (1995) (blue) yield sets. **Left**: IMF-integrated nitrogen-to-oxygen yield ratios computed with VICE for the same studies. The Limongi & Chieffi (2018) yields are calculated with progenitor rotational velocities of $v_{\rm rot} = 0$ (circles), 150 (triangles), and 300 km/s (stars). All other studies only report yields for non-rotating progenitors.

The flat, dotted black line denotes $\log_{10}(\rm N/O)_{\rm CC}$ = -1.5, the value empirically derived from observations (Vincenzo et al., 2016; Berg et al., 2012; Izotov et al., 2012; James et al., 2015). The rotating progenitor models from Limongi & Chieffi (2018) do the best job of reproducing this ratio in theoretical models of core collapse supernova ejecta; the other models do not include rotation, which appears to play a key role in establishing this empirical result.

What is the implied plateau in [N/O]?

[N/O] and log(N/O) are directly related, but one is relative to the sun while the other is just a ratio of number densities. Expanding [N/O]:

$$[\rm N/O] = [\rm N/H] - [\rm O/H] \tag{4a}$$

$$= \log_{10}\left(\frac{Z_{\rm N}}{Z_{\rm N,\odot}}\right) - \log_{10}\left(\frac{Z_{\rm O}}{Z_{\rm O,\odot}}\right) \tag{4b}$$

$$= \log_{10}\left(\frac{Z_{\rm N}}{Z_{\rm O}}\right) - \log_{10}\left(\frac{Z_{\rm N,\odot}}{Z_{\rm O,\odot}}\right) \tag{4c}$$

Zooming in on the $Z_{\rm N}/Z_{\rm O}$ term:

$$\log_{10}\left(\frac{Z_{\rm N}}{Z_{\rm O}}\right) = \log_{10}\left(\frac{\mu_{\rm N} n_{\rm N}}{\mu_{\rm O} n_{\rm O}}\right) \tag{5a}$$

$$= \log_{10}\left(\frac{\mu_{\rm N}}{\mu_{\rm O}}\right) + \log_{10}\left(\frac{n_{\rm N}}{n_{\rm O}}\right) \tag{5b}$$

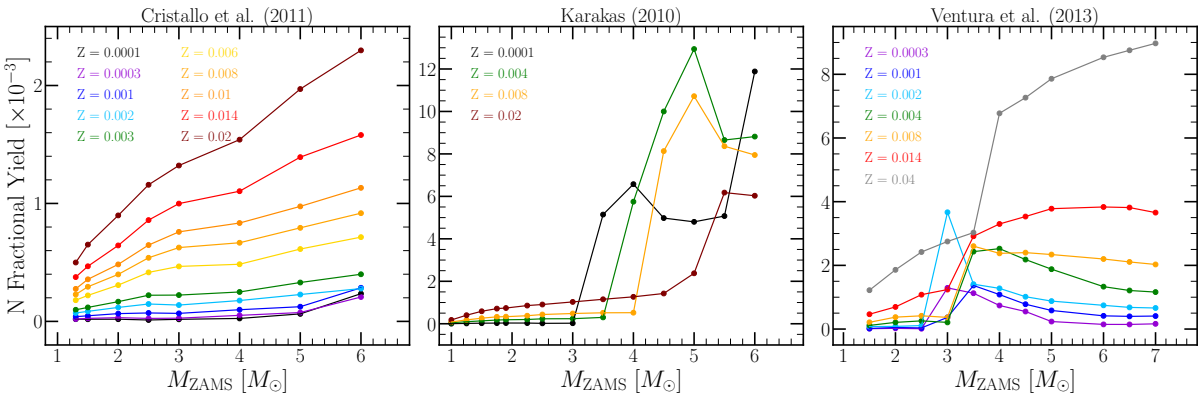

Figure 2: Fractional yields of N as a function of progenitor zero age main sequence mass at the metallicities at which Cristallo et al. (2011) (left), Karakas (2010) (middle), and Ventura et al. (2013) (right) report yields.

where μ and n are again the mean molecular weight and number of some species x. The term $\log_{10}(n_{\rm N}/n_{\rm O})$ is exactly the log(N/O) value which Berg et al. (2012), Izotov, Thuan & Guseva (2012), and James et al. (2015) measured to be ∼-1.5. Plugging this in:

$$[{\rm N/O}] = \log_{10}\left(\frac{\mu_{\rm N}}{\mu_{\rm O}}\right) + \log_{10}\left(\frac{n_{\rm N}}{n_{\rm O}}\right) - \log_{10}\left(\frac{Z_{\rm N,\odot}}{Z_{\rm O,\odot}}\right) \tag{6a}$$

Taking $\mu_{\rm N} = 14.007$ and $\mu_{\rm O} = 15.999$ again, with the empirical result of $\log_{10}(n_{\rm N}/n_{\rm O}) = $ -1.5 and the Asplund et al. (2009) solar photospheric composition of $Z_{\rm N,\odot} = 6.91\times10^{-4}$ and $Z_{\rm O,\odot} = 0.00572$, yields the following:

$$[{\rm N/O}]_{\rm plateau} = -0.64 \tag{7}$$

Asymptotic Giant Branch Star Yields

Figure 2 presents the fractional yields of N as a function of progenitor zero age main sequence (ZAMS) mass and metallicity as reported in the FRUITY database (Cristallo et al., 2011, 2015, left), by Karakas (2010) (middle), and by Ventura et al. (2013) (right). All models predict a metallicity dependence to the nitrogen yields, though with noticeably different dependencies; both Cristallo et al. (2011, 2015) and Ventura et al. (2013) predict the yields to increase more or less linearly with progenitor metallicity, whereas the Karakas (2010) yields predict higher N yields at lower metallicities for higher mass AGB stars. This is a consequence of the interplay between third dredge up (TDU) and hot bottom burning (HBB) in these models.

TDU refers to the repeated penetrations of the convective envelope into the hydrogen depleted core during the thermal pulses associated with AGB star evolution. This process is particularly important in low mass AGB stars whose main source of neutrons is the ^{13}C(α, n)^{16}O reaction, which can occur at substantial rates when C is mixed with material from the He-rich shell during each TDU episode. At solar metallicity, Karakas (2010) suggests that only stars with $M_{\rm ZAMS} \gtrsim 2.5\ M_\odot$ are massive enough to experience TDU, though the threshold is as low as $\sim 1\ M_\odot$ at $Z \approx 10^{-4} Z_\odot$; lower mass stars instead experience only a core

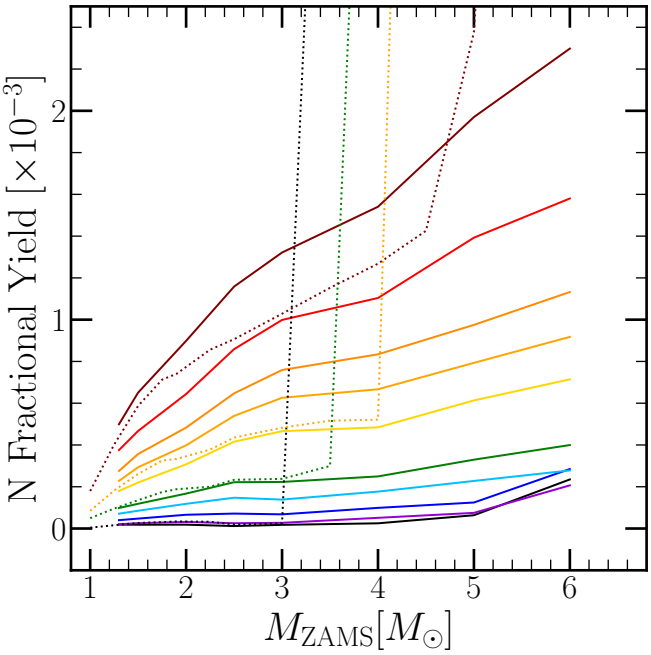

Figure 3: The same as figure 2, but with the Cristallo et al. (2011) (solid) and Karakas (2010) (dotted) yields plotted on the same set of axes for comparison.

helium flash. HBB refers to proton captures at the base of the convective envelope, which activates the CNO cycle, producing large amounts of ^{13}C and ^{14}N. It requires temperatures of at least 30-40 MK according to Ventura et al. (2013), but 80 MK according to Cristallo et al. (2015). HBB requires a higher mass AGB progenitor (∼4 - 5 $M_{\odot}$), but like TDU, the minimum mass also decreases at lower progenitor metallicity. The CNO cycle:

^{12}C(p,γ)^{13}N(β^{+}, ν_e)^{13}C(p,γ)^{14}N(p,γ)^{15}O(β^{+}, ν_e)^{15}N(p,α)^{12}C

The most efficient N production thus occurs when an AGB star experiences *both* TDU and HBB, because each TDU episode adds more C and N seed nuclei with which to conduct p-capture nucleosynthesis. This is the reason the Karakas (2010) N yields are so high at high masses: every massive star in their model experiences both TDU and HBB, whereas the Ventura et al. (2013) models have both only in the ∼3 - 4 $M_{\odot}$ range (hence the enhanced N yields there). The Cristallo et al. (2011) paper makes no mention of HBB, but my impression from Cristallo et al. (2015) is that their $M > 4$ $M_{\odot}$ models all have both TDU and HBB implemented, though in most cases one is much more efficient than the other. The metallicity dependence of the N yields reported by Karakas (2010) therefore reflect the fact that low-Z models experience deeper TDU and stronger HBB (see discussion in § 4.1 of Ventura et al., 2013). Beyond this, a direct comparison of the models is significantly challenging (and even avoided by mose of the papers which publish them) owing to the laundry list of assumptions that go into the stellar models: the treatment of convection and convective boundaries, the mass-loss rate, opacities, the equation of state, the nuclear reaction network, etc.

How consistent are Cristallo et al. (2011, 2015) and Karakas (2010) up to ∼3 - 4 $M_\odot$? Figure 3 compares the two sets of yields on the same plot, with the Cristallo et al. (2011, 2015) set shown in solid lines and the Karakas (2010) set in dotted lines. The two are broadly consistent with one another up to this threshold mass, at which point HBB takes hold in the Karakas (2010) model, significantly enhancing the N yields for higher mass progenitors.

Analytic Motivation of Nitrogen Yields

Can we come up with a mathematical framework with which to relate a late-time [N/O]-[O/H] relation and nitrogen yields using equilibrium arguments in simple one-zone models?

The time-derivative of the main sequence mass fraction

The main sequence mass fraction is the fraction of a stellar population's mass still on the main sequence. If the post-main sequence lifetime is approximated to be zero, this is also the star cluster mass fraction. It is given by:

$$h = \frac{\int_l^{m_{\rm to}} m \frac{dN}{dm} dm}{\int_l^u m \frac{dN}{dm} dm}, \tag{8}$$

where l and u are the lower and upper mass limits on star formation, respectively, dN/dm is the adopted stellar IMF, and $m_{\rm to}$ is the turnoff mass in solar masses. Allowing the constant ξ to represent the normalization of the IMF, zooming in on the denominator:

$$\int_l^u = \xi m^{1-\alpha} dm \tag{9a}$$

$$= \frac{\xi}{2-\alpha} m^{2-\alpha}\Big|_l^u \tag{9b}$$

$$= \frac{\xi}{0.7} m^{0.7}\Big|_{0.08}^{0.5} - \frac{\xi}{0.6} m^{-0.3}\Big|_{0.5}^{100} \tag{9c}$$

$$= 2.239\xi \tag{9d}$$

where the power-law indeces and constants are appropriate for a Kroupa (2001) IMF (with 0.6 in the second denominator rather than 0.3 to account for piece-wise continuity) assuming l = 0.08 and u = 100. In the numerator of h, only the quantity $m_{\rm to}$ varies with time. The time-derivative then follows trivially from the stellar IMF.

$$\dot{h} = \frac{1}{2.239\xi} \frac{d}{dt} \int_l^{m_{\rm to}} m \frac{dN}{dm} dm \tag{10a}$$

$$= \frac{1}{2.239\xi} \frac{d}{dm_{\rm to}} \int_l^{m_{\rm to}} m \frac{dN}{dm} dm \frac{dm_{\rm to}}{dt} \tag{10b}$$

$$= \frac{m_{\rm to}}{2.239\xi} \frac{dN}{dm}\Big|_{m_{\rm to}} \frac{dm_{\rm to}}{dt} \tag{10c}$$

$$= \frac{m_{\rm to}}{2.239\xi} A\xi m_{\rm to}^{-\alpha} \frac{dm_{\rm to}}{dt} \tag{10d}$$

where $\alpha = 1.3$ (2.3) for $0.08 \leq m \leq 0.5$ ($m \geq 0.5$) according to the Kroupa (2001) IMF and $A = 1$ (0.5) for the same mass ranges ensures piece-wise continuity of the IMF. However, since the lifetime of an $m = 0.5$ star is very long (∼113 Gyr for `VICE`'s approximation), $A = 0.5$ and $\alpha = 2.3$ always for the sake of this calculation.

$$= \frac{0.5 m_{\rm to}}{2.239\xi} \xi m_{\rm to}^{-2.3} \frac{dm_{\rm to}}{dt} \tag{11a}$$

$$= 0.223 m_{\rm to}^{-1.3} \frac{dm_{\rm to}}{dt} \tag{11b}$$

The turnoff mass at a given time, as approximated in `VICE`, is given by

$$m_{\rm to} = \left(\frac{t}{\tau_\odot}\right)^{-1/3.5} = \left(\frac{t}{\tau_\odot}\right)^{-2/7}, \tag{12}$$

where $\tau_\odot$ is the main sequence lifetime of the sun. Differentiating with time:

$$\frac{dm_{\rm to}}{dt} = \frac{-2}{7\tau_\odot}\left(\frac{t}{\tau_\odot}\right)^{-9/7} \tag{13}$$

Plugging equations 12 and 13 into equation 11b:

$$\dot{h} = 0.223 \left(\frac{t}{\tau_\odot}\right)^{2.6/7} \left(\frac{-2}{7\tau_\odot}\right) \left(\frac{t}{\tau_\odot}\right)^{-9/7} \tag{14a}$$

$$= \frac{-0.0637}{\tau_\odot}\left(\frac{t}{\tau_\odot}\right)^{-6.4/7} \tag{14b}$$

$$= \frac{-0.0637}{\tau_\odot}\left(\frac{t}{\tau_\odot}\right)^{-32/35} \tag{14c}$$

This form for $\dot{h}$ is appropriate for the Kroupa (2001) IMF with a mass range of star formation defined by $l = 0.08$ and $u = 100$ assuming a mass-lifetime relationship given by 12. However, the time-dependence is set not by the IMF but by the mass-lifetime relationship; the IMF affects only the normalization of $\dot{h}$.

The Enrichment Rate from AGB Stars

Next, equation 14c must be plugged into the equation describing the enrichment rate from AGB stars:

$$\dot{M}_{\rm N}^{\rm AGB} = -\int_0^T y_{\rm N}^{\rm AGB}(m_{\rm to}(T-t), Z_{\rm ISM}(t))\dot{M}_\star(t)\dot{h}(T-t)dt \tag{15}$$

In general, the SFR $\dot{M}_\star$ can have any time-dependence, and the gas-phase abundance of the star forming reservoir $Z_{\rm ISM}$ as a function of time has some complicated form which depends on the SFH. As a first guess though, we can assume a constant SFR, and since nitrogen production is dominated by young stellar populations, most of the enrichment should be coming from stars near the equilibrium abundance. Furthermore, the AGB star yields of N appear to depend more or less linearly on initial stellar mass. As a first guess then, assume

that $y_{\rm N}^{\rm AGB} = \xi m_{\rm to} Z$ where ξ is simply a normalizing constant. Under these assumptions this integral can be re-expressed as:

$$\dot{M}_{\rm N}^{\rm AGB} = -\int_0^T \xi m_{\rm to}(T-t) Z_{\rm eq} \dot{M}_\star \dot{h}(T-t) dt \tag{16a}$$

$$= \xi Z_{\rm eq} \dot{M}_\star \int_0^T \left(\frac{T-t}{\tau_\odot}\right)^{-2/7} \frac{0.0637}{\tau_\odot} \left(\frac{T-t}{\tau_\odot}\right)^{-6.4/7} dt \tag{16b}$$

$$= \frac{0.0637 \xi Z_{\rm eq} \dot{M}_\star}{\tau_\odot} \int_0^T \left(\frac{T-t}{\tau_\odot}\right)^{-8.4/7} dt \tag{16c}$$

$$= \frac{0.0637 \xi Z_{\rm eq} \dot{M}_\star}{\tau_\odot} \left[\left(\frac{-7}{1.4}\right)\left(\frac{T-t}{\tau_\odot}\right)^{-1.4/7} (-\tau_\odot)\right]_0^T \tag{16d}$$

$$= 0.3185 \xi Z_{\rm eq} \dot{M}_\star \left[\left(\frac{\tau_8}{\tau_\odot}\right)^{-1.4/7} - \left(\frac{T}{\tau_\odot}\right)^{-1.4/7}\right] \tag{16e}$$

$$= 0.3185 \xi Z_{\rm eq} \dot{M}_\star \left[\left(\frac{\tau_8}{\tau_\odot}\right)^{-1.4/7} - \left(\frac{T}{\tau_\odot}\right)^{-1.4/7}\right] \tag{16f}$$

$$= 1.064 \xi Z_{\rm eq} \dot{M}_\star \tag{16g}$$

In the second to last equality, the upper bound of the integral is evaluated at $T - \tau_8$ rather than inserting an infinity; mathematically, the infinite value reflects the divergence of $\dot{h}$ for zero-age stellar populations. However, the integral really should only be evaluated up to the simulation time minus the lifetime of an 8 $M_\odot$ star (τ_8), since these are the most massive AGB stars in these models. The final equality assumes a lifetime of $\tau_\odot 8^{-3.5}$ Gyr as the lifetime of an 8 $M_\odot$ star, $T = 13.2$ Gyr as the simulation time, and $\tau_\odot = 10$ Gyr as the lifetime of the sun.

The rate of CCSN enrichment reflects the yield at the equilibrium metallicity:

$$\dot{M}_{\rm N}^{\rm CC} = y_{\rm N}^{\rm CC}(Z_{\rm eq}) \dot{M}_\star \tag{17}$$

The Equilibrium Abundance of Nitrogen

The equilibrium metallicity for a constant SFH then corresponds to solving for $\dot{Z}_{\rm N} = 0$ from the following, derived from the enrichment equation and the equilibrium arguments from Weinberg, Andrews & Freudenburg (2017):

$$\dot{Z}_{\rm N} = \frac{1}{\dot{M}_\star \tau_\star}\left[\dot{M}_{\rm N}^{\rm CC} + \dot{M}_{\rm N}^{\rm AGB} - Z_{\rm N}\dot{M}_\star(1+\eta-r)\right] \tag{18}$$

When $\dot{Z}_{\rm N} = 0$, $Z_{\rm N} = Z_{\rm N,eq}$, the equilibrium abundance of nitrogen. It then follows:

$$Z_{\rm N,eq}\dot{M}_\star(1+\eta-r) = \dot{M}_{\rm N}^{\rm CC} + \dot{M}_{\rm N}^{\rm AGB} \tag{19a}$$

$$= y_{\rm N}^{\rm CC}(Z_{\rm eq})\dot{M}_\star + 1.064\xi Z_{\rm eq}\dot{M}_\star \tag{19b}$$

$$Z_{\rm N,eq} = \frac{y_{\rm N}^{\rm CC}(Z_{\rm eq}) + 1.064\xi Z_{\rm eq}}{1+\eta-r} \tag{19c}$$

Since nitrogen has metallicity dependent yields, $Z_{\rm eq}$ is the *total* abundance. The constant ξ specifies the normalization of the nitrogen AGB star yield assuming a linear dependence on both turnoff mass and metallicity given by $y_{\rm N}^{\rm AGB} = \xi m_{\rm to} Z$. This form does make the assumption that all AGB star production is coming from younger stellar populations near the equilibrium abundance. Since N production timescales are quite short ($\sim$100 Myr), this assumption is likely accurate enough. The constant ξ could be determined by a fit to the Cristallo et al. (2011) or the Ventura et al. (2013) models, also absorbing whatever prefactor is built in; the Karakas (2010) yields likely couldn't be used for this since they do not show a linear dependence of $y_{\rm N}^{\rm AGB}$ on progenitor mass.

The basic motivation of this is that at a given radius $R_{\rm gal}$, the equilibrium abundance of oxygen is known by the scaling of η to set the metallicity gradient. By assuming that the equilibrium abundance of nitrogen reflects the observed [N/O]-[O/H] relation, the only remaining unknowns in this formalism are the yields. This procedure can then be tested with `VICE`'s numerical simulations allowing migration, time-dependent SFHs, etc. to test how robust the predictions are to the assumptions built into this analytic argument.

Single Stellar Population Production of Nitrogen

Production Timescales Relative to Fe

Using $y_{\rm N}^{\rm CC} = 5 \times 10^{-4}$, the AGB star yields of N from the FRUITY database (Cristallo et al., 2011), and supernova yields of Fe as in Johnson & Weinberg (2020) and Weinberg et al. (2017) (i.e. $y_{\rm Fe}^{\rm CC} = 0.0012$ and $y_{\rm Fe}^{\rm Ia} = 0.0017$), **what is the net production of N and Fe as a function of stellar population age and metallicity?**

The left-hand panel of Figure 4 shows the net production of N and Fe as a function of stellar population age and metallicity. Since Fe has metallicity-independent yields under these assumptions, it's plotted with only one curve, whereas N has different production timescales at different metallicities. In general, the CCSN yields of N under these assumptions make up a substantially larger fraction of the N production than the CCSN yields of Fe does for its production. This means that the characteristic timescales for N production are significantly shorter than for Fe.

The AGB yields of N are also significantly weighted toward high masses such that even at solar metallicity, $\gtrsim$90% of the N production is complete by the time the population is $\tau =$ 1 Gyr old. Although the fractional yields are higher for more massive AGB stars, this does not mean that the total N produced in low-mass AGB stars is lower than that produced by high mass AGB stars due to the steep nature of the initial mass function. In a window of progenitor mass $[m,\, m + dm]$ at a metallicity Z, the total mass of N produced is given by:

$$dm_{\rm N} = y(m|Z) m \frac{dN}{dm} = y(m|Z) \xi m^{1-\alpha} \tag{20}$$

where α is the power-law index of the IMF. If the production at two masses m_1 and m_2 are comparable, then the scaling of the yield y with progenitor mass can be derived:

$$dm_{\rm N}|_{m=m_1} = dm_{\rm N}|_{m=m_2} \tag{21a}$$

$$\implies y(m_1|Z) \xi m_1^{1-\alpha} = y(m_2|Z) \xi m_2^{1-\alpha} \tag{21b}$$

$$\implies \frac{y(m_1|Z)}{y(m_2|Z)} = \left(\frac{m_1}{m_2}\right)^{\alpha - 1} \tag{21c}$$

If the yield y scales with $m^{-\gamma}$ and the IMF-integrated mass production is to be mass-independent, then $\gamma = 1 - \alpha =$ -1.3. Only when $y \propto m^{1.3}$ will the IMF-integrated contribution of high mass stars be comparable to that of low-mass stars. The weight of low-mass stars increases with increasing γ, and conversely for high-mass stars with decreasing γ. Based on these investigations of the Cristallo et al. (2011) yields (see `latex/yields/yields.pdf`), it appears that $\gamma \approx$ -1 for nitrogen (if anything else, the $y - m$ relation appears to me that it might be slightly sub-linear), indicating that the IMF-integrated production is marginally dominated by low-mass stars.

Isolating the AGB Star Contribution

To isolate the AGB star contribution to single stellar population production of iron and nitrogen, $y_{\rm N}^{\rm CC}$ and $y_{\rm Fe}^{\rm CC}$ were both set to zero, and `VICE`'s `single_stellar_population` function reran at the same metallicities as in the left-hand panel of Figure 4; the results are shown in the right-hand panel. Points are plotted at the top of the panel to denote when 50% of

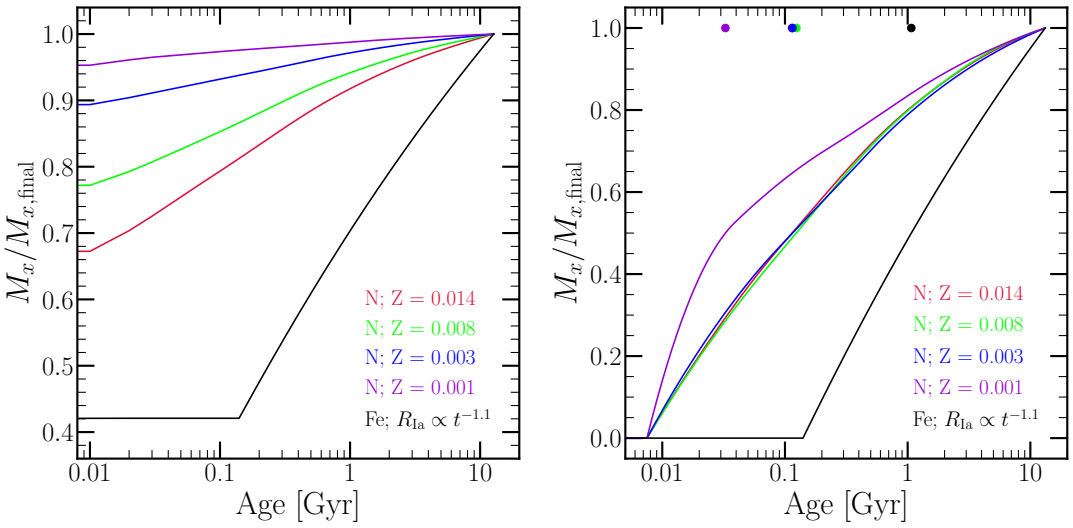

Figure 4: **Left**: Net mass of N (colored lines) and Fe (black) as a function of stellar population age and metallicity (color-coded according to legend for N), in units of the mass produced at $\tau = 12.2$ Gyr. **Right**: The same as the left, but with the core collapse supernova yields of both N and Fe set to zero. The points at the top denote the time at which 50% of the yield at $\tau = 13.2$ Gyr has been produced.

the yield is produced. Clearly, nitrogen production occurs on average an order of magnitude sooner than iron production - in most cases before the SN Ia DTD even begins.

How can the production be dominated by high-mass stars if the IMF-integrated yields are dominated by low-mass stars? To understand this, it is enlightening to consider the scenario in which the production of some element x in AGB stars is time-independent. That is,

$$\dot{M}_x^{\mathrm{AGB}} = \text{constant} \tag{22}$$

Under this assumption, in any time interval from τ to $\tau + d\tau$, the amount of production of some element x is always the same. This corresponds to an idealized scenario in which stars of all masses contribute equally to enrichment when stellar lifetimes are taken into account. The question then becomes, **what is the required dependence of the AGB yield on mass at a given metallicity for the production rate to be constant?** For this calculation, we'll assume the IMF, lifetime, and yield scale with progenitor stellar mass m in the following way:

$$\frac{dN}{dm} \propto m^{-\alpha} \tag{23a}$$

$$\tau \propto m^{-\beta} \tag{23b}$$

$$y \propto m^{-\gamma} \tag{23c}$$

where to answer this question we will need to calculate the appropriate value of γ.

The rate of production of some element x can be expressed according to:

$$\dot{M}_x^{\rm AGB} = y(m_{\rm to}|Z) M_\star \dot{h} \tag{24}$$

where $y(m_{\rm to}|Z)$ is the yield at the main sequence turnoff mass at some metallicity Z, $M_\star$ is the total initial mass of the progenitor stellar population, and $\dot{h}$ is the time-derivative of the *main sequence mass fraction* (see Johnson & Weinberg (2020), or section 3 of VICE's science documentation[1]). In detail, VICE takes into account post main-sequence lifetimes by simply inflating the lifetime τ by some amount (10% by default), but for the purposes of this calculation, I'm assuming it to be zero. It is defined by:

$$h = \frac{\int_l^{m_{\rm to}} m \frac{dN}{dm} dm}{\int_l^u m \frac{dN}{dm} dm} \tag{25}$$

where l and u are the lower and upper mass limits of star formation, respectively, and dN/dm is the IMF. Taking the time-derivative of h may appear non-trivial, but it is simplified greatly by the usage of the chain rule and the fundamental theorem of calculus. Conventiently, the demoninator of h is simply the initial mass of the stellar population and is time-independent; for ease, I'll denote it here simply as $M_\star$.

$$\dot{h} = M_\star^{-1} \frac{d}{dm_{\rm to}} \left(\int_l^{m_{\rm to}} m \frac{dN}{dm} dm \right) \frac{dm_{\rm to}}{d\tau} \tag{26a}$$

$$= M_\star^{-1} m_{\rm to} \frac{dN}{dm}\Big|_{m_{\rm to}} \frac{dm_{\rm to}}{d\tau} \tag{26b}$$

$$\propto M_\star^{-1} m_{\rm to}^{1-\alpha} \frac{d}{d\tau} (\tau^{-1/\beta}) \tag{26c}$$

$$\propto M_\star^{-1} m_{\rm to}^{1-\alpha} \frac{-1}{\beta} \tau^{-(1+\beta)/\beta} \tag{26d}$$

$$\propto M_\star^{-1} \tau^{(\alpha-1)/\beta} \frac{-1}{\beta} \tau^{-(1+\beta)/\beta} \tag{26e}$$

$$\propto M_\star^{-1} \frac{-1}{\beta} \tau^{(\alpha-2-\beta)/\beta} \tag{26f}$$

Therefore, under this formalism, the main sequence mass fraction should decrease monotonically with time (as expected) according to $\dot{h} \sim \tau^{(\alpha-2-\beta)/\beta}$.

Next, if the yield y scales with $m_{\rm to}^{-\gamma}$, then it should scale with time according to $y \sim \tau^{\gamma/\beta}$. Plugging all of this in yields the following time-dependence for the AGB enrichment rate:

$$\dot{M}_x^{\rm AGB} \sim \tau^{\gamma/\beta} \tau^{(\alpha-2-\beta)/\beta} \tag{27a}$$

$$= \tau^{(\alpha+\gamma-2-\beta)/\beta} \tag{27b}$$

and if the enrichment rate is to be a constant, the power-law index must be equal to zero:

$$\alpha + \gamma - 2 - \beta = 0 \implies \gamma = 2 + \beta - \alpha \tag{28}$$

[1] https://vice-astro.readthedocs.io/en/latest/science_documentation/SSPs/index.html

If $\alpha = 2.3$ and $\beta = 3.5$, as adopted in VICE, then $\gamma = 3.2$. If all stellar masses are to contribute equally to the AGB enrichment rate when lifetimes are taken into account such that the rate is constant, then the yields must increase sharply with decreasing stellar mass. I note that the high value of γ is truly a consequence of the high value of β ($2 - \alpha$ = -0.3). Under this parameterization, for higher values of γ, the AGB enrichment rate increases with time as the yields of low-mass stars become more and more important. For lower values, the production rate falls with time due to the lifetimes of low-mass stars preventing them from producing yields quickly enough to maintain a constant production rate. This is an indication that even though the IMF-integrated AGB stars yields of N are marginally weighted toward low-mass AGB stars, the amount which is produced on the order of a hubble time will be dominated by high mass stars unless the yields have a very strong, inverse dependence on progenitor stellar mass.

Which Set of AGB Star Yields?

Between the Cristallo et al. (2011), Karakas (2010), and Ventura et al. (2013) tables, which one performs better? Several steps are required to address this question, the first of which is simply assessing the predicted nitrogen yield from single stellar population models as a function of progenitor metallicity. This calculation is shown in Fig. 5, where the total nitrogen yield from AGB stars only is plotted as a function of progenitor metallicity for hypothetical 13.2 Gyr old stellar populations. Generally, the Cristallo et al. (2011) and Ventura et al. (2013) yields suggest similar nitrogen production as a function of progenitor metallicity, up to a normalization constant. The Karakas (2010) yields, however, suggest a different trend with progenitor metallicity. This raises the question of whether or not the Karakas (2010) yields will be able to reproduce the observed [N/O]-[O/H] relation, which strongly suggests *increasing* nitrogen yields with increasing progenitor metallicity, as supported by the Cristallo et al. (2011) and Ventura et al. (2013) tables.

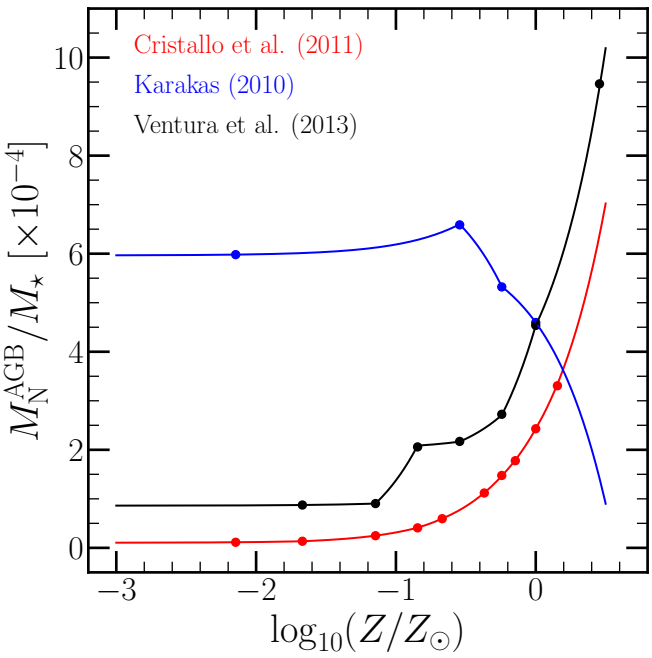

Figure 5: Total nitrogen production by AGB stars from a hypothetical 13.2 Gyr old stellar population as a function of progenitor metallicity; only AGB stars have non-zero yields in this calculation. Curves show the predicted nitrogen production normalized by the initial mass of the stellar population assuming the Cristallo et al. (2011) (red), Karakas (2010) (blue), and Ventura et al. (2013) (black) tables. Points are plotted at the metallicities at which each study has reported yields.

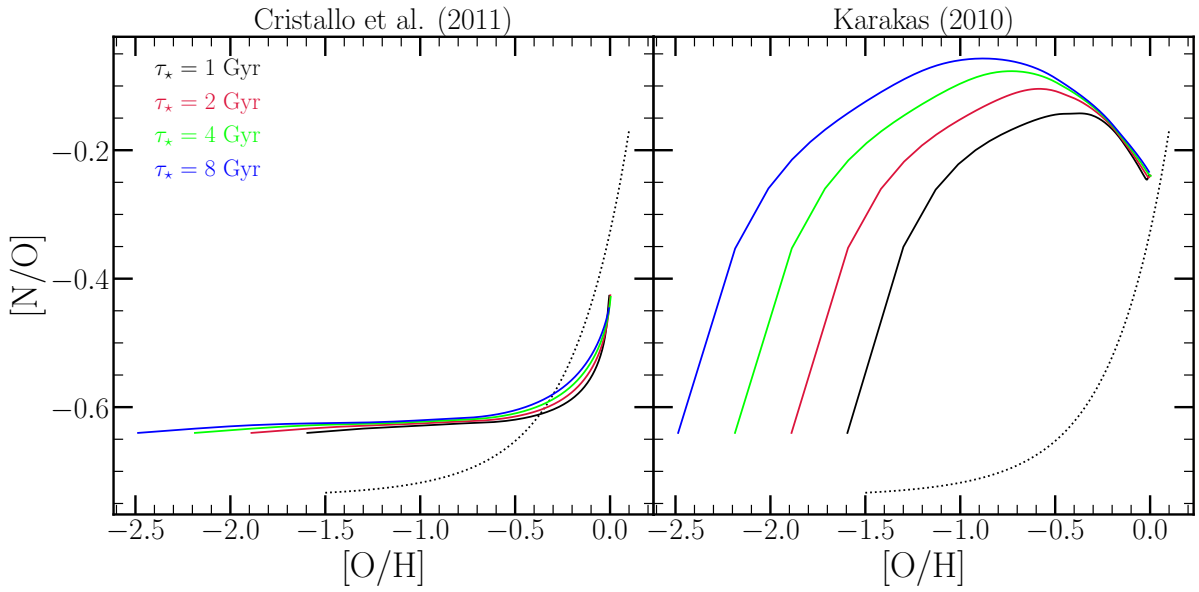

Figure 6: [N/O]-[O/H] tracks as predicted by Cristallo et al. (2011) (left) and Karakas (2010) (right). Colored lines denote different SFE timescales denoted in the legend in the upper left. The black dotted line denotes the fit to the observed [N/O]-[O/H] relation published in Henry, Edmunds & Köppen (2000).

One-Zone Models

The Impact of the AGB Star Yields

How do the abundances predicted by one-zone models differ between the Cristallo et al. (2011) and Karakas (2010) yield sets?

Taking $\dot{M}_\star$ = constant, $\eta = 2.0$, and $y_{\rm N}^{\rm CC} = 4.15 \times 10^{-4}$ as suggested by supernova yields and the observed [N/O] plateau at low [O/H], the [N/O]-[O/H] tracks for $\tau_\star = 1$, 2, 4, and 8 Gyr for both studies is shown in Fig. 6. The black dotted line denotes the population-averaged trend published in Henry, Edmunds & Köppen (2000). The model recovers the qualitative observational trend with the Cristallo et al. (2011) yields, though the increase in [N/O] at high [O/H] isn't as large as in the observations. The Karakas (2010) yields predict a trend in tension with the observations, but this makes sense when considering how these yields depend on mass and metallicity (see Fig. 2). Their highest yields are for higher mass stars at low metallicity; although the Cristallo et al. (2011) yields also predict the yields to increase with stellar mass, the metallicity trend appears to be what's most important here. At early times when [O/H] is low, the high mass AGB stars dump a lot of N, getting the ISM off the plateau more or less immediately. The peak and subsequent decrease in [N/O] at high [O/H] can be understood from the decrease in the N yields near solar Z as reported by Karakas (2010).

Since the Cristallo et al. (2011) yields recover the correct trend, but the Karakas (2010) yields appear to have a more realistic magnitude, better agreement with the observations can be achieved by simply amplifying the Cristallo et al. (2011) yields by some factor; this is demonstrated in Fig. 7. The model with amplified yields agrees with the observational

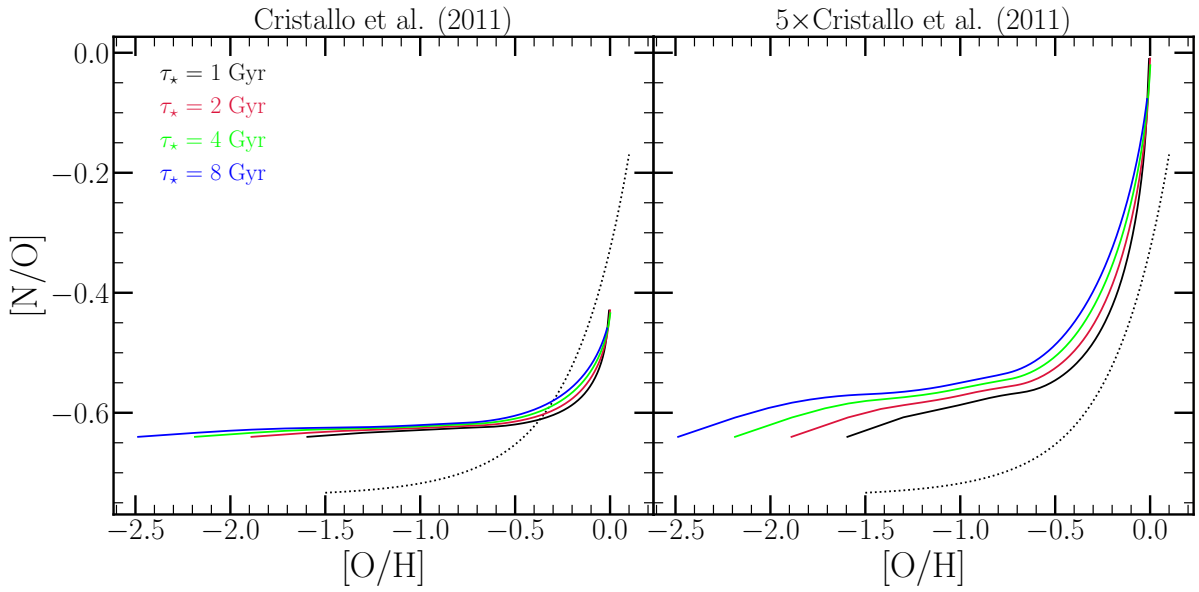

Figure 7: [N/O]-[O/H] tracks as predicted with the Cristallo et al. (2011) yields (left), and with the same yield set but amplified by a factor of 5 (right).

result better, even though it overestimates [N/O] and all [O/H]. A better match could be achieved by lowering $y_{\rm N}^{\rm CC}$, which predicts a plateau at a marginally higher [N/O] than Henry, Edmunds & Köppen (2000). Nonetheless, this is a good demonstration that even taking the more realistic of the two yield sets, the yields must be artificially amplified by a substantial prefactor in order to predict ∼solar [N/O] at ∼solar [O/H]. **This re-raises the question of the timescales of N enrichment from a single stellar population: if AGB stars make up a more substantial fraction of the nitrogen enrichment in the universe, will that increase the characteristic delay times of nitrogen production seen with the base set of yields from Cristallo et al. (2011)? This should impact the amplitude of variability in its production.**

Multi-Zone Milky Way Models

The Resultant [N/O]-[O/H] Relation

Any viable model for nitrogen production in the Milky Way must accurately reproduce the observed abundances and their correlations with other elements. **Here we test a fiducial model for nitrogen yields.** The model has $y_{\rm N}^{\rm CC} = 4.15 \times 10^{-4}$, $y_{\rm N}^{\rm Ia} = 0$, and $y_{\rm N}^{\rm AGB}$ described by the Cristallo et al. (2011) yields amplified by a factor of 5. Otherwise, the model is the same as the inside-out SFH model with diffusion migration from Johnson et al. (2021). Its predictions for the present day are shown in comparison to observational samples from a wide variety of astrophysical environments in Fig. 8. As discussed in Vincenzo et al. (2016), the observed [N/O]-[O/H] relation is more or less universal between systems; the comparison to the Dopita et al. (2016) measurements further suggests that this extends to high redshift as well (z $\sim$ 3). It also appears to be relatively independent of the measurement method.

For the fiducial model, each individual annulus at $R_{\rm gal} \geq 2$ kpc is represented by a point on the line. In general, it is more linear than the observed data. This suggests that at high metallicities, the model is under-predicting nitrogen production relative to oxygen, whereas it over-predicts it at low abundances. Since stellar migration only induces variability in $\dot{Z}_{\rm x}$ for some element x with delayed enrichment and only affects the time-averaged trend at large $R_{\rm gal}$ and early times, the late-time abundances should be reasonably described by the late-time equilibrium abundance of a one-zone model with similar parameters as one of the rings at a given $R_{\rm gal}$. Multiple studies focusing on the yields of AGB stars suggest that the nitrogen yields should depend more or less linearly on the initial mass of the progenitor (Cristallo et al., 2011; Ventura et al., 2013), although the tables published by Karakas (2010) provide circumstantial evidence that they could be much higher for the most massive AGB stars, particularly at low metallicity. Since these studies largely agree on this qualitative result, the simplest way to recalibrate the yields is most likely by adjusting $y_{\rm N}^{\rm CC}$ and its dependence on Z, whose values span a much wider dynamic range between the Limongi & Chieffi (2018), **?**, Nomoto, Kobayashi & Tominaga (2013), and Woosley & Weaver (1995) results.

Is the resultant [N/O]-[O/H] relation a superposition of endpoints? This question is addressed in Fig. 9, which plots the present-day [N/O]-[O/H] relation in the gas-phase (parameterized by radius) as well as the evolutionary tracks (parameterized by time) for a selection of radii in the model. This is shown for the Cristallo et al. (2011) (left), Karakas (2010) (middle), and Ventura et al. (2013) (right) AGB star yields. As in previous versions of this model, the Cristallo et al. (2011) yields have been amplified by a factor of 5 to improve agreement with the observed abundances; although this isn't the case for the Ventura et al. (2013) yields, it's likely they'll need amplified as well. In the Cristallo et al. (2011) and Ventura et al. (2013) models, the relation arises out of a series of end-points, having a slightly shallower slope than the relation predicted by the evolutionary track of a one-zone model. The Karakas (2010) yields disagree with this prediction; in that model, the trend arises out of the metallicity dependence of the yields alone - the evolutionary tracks for individual annuli nearly overlap. However, the Karakas (2010) model fails to reproduce the observed trend. Instead, it predicts a trend which is nearly flat at low [O/H], then decreases monotonically at [O/H] $\gtrsim$ 0. This is in tension with the observed trend, with the [N/O] abundances at low [O/H] in tension with the observations at the $\sim$0.5 dex level.

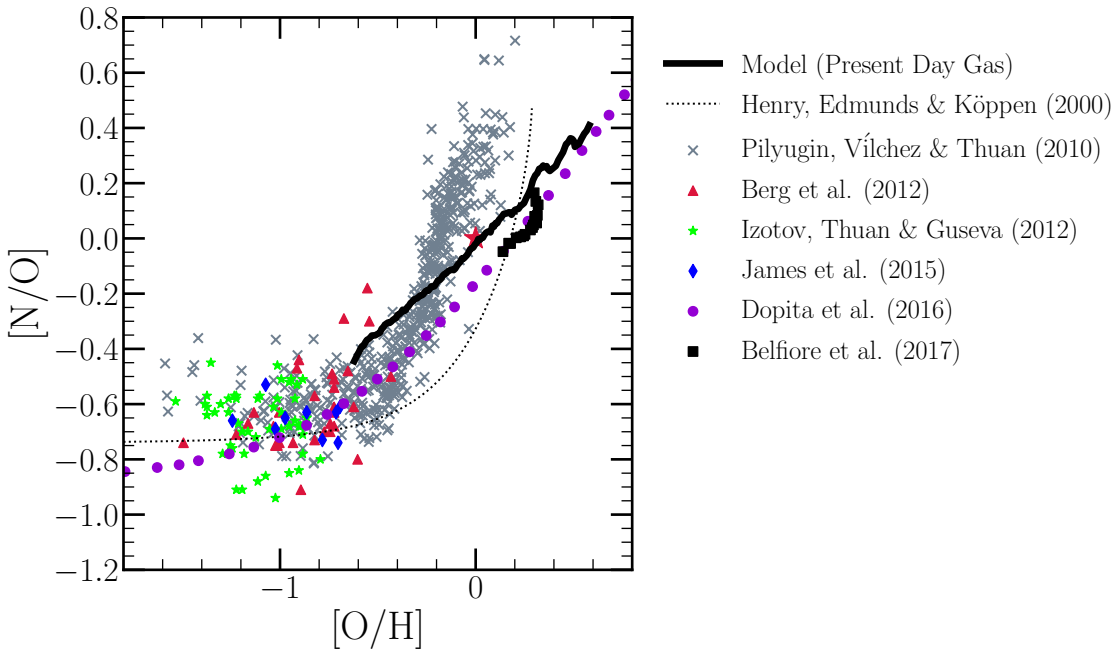

Figure 8: Observational results on the gas-phase [N/O]-[O/H] relation in comparison with a fiducial model at the present day (solid, thick black line). For the fiducial model, each individual ring at a radius of $R_{\rm gal} \geq 2$ kpc is plotted as a point on the line. The sun (at (0, 0) by definition) is plotted in a large red star. The fit to an analytic chemical evolution model using data from Galactic HII regions, main sequence and halo stars, and damped lyman alpha systems from Henry et al. (2000) is shown in a dotted black line. Abundances derived from electron temperatures of HII in nearby NGC spiral galaxies at shown in grey X's (Pilyugin, Vílchez & Thuan, 2010). Measurements from blue, star forming diffuse dwarf galaxies probing the low metallicity regime are shown in red triangles (Berg et al., 2012), green stars (Izotov, Thuan & Guseva, 2012), and blue diamonds (James et al., 2015). The N/O vs. O/H calibration derived from local stars and HII regions from Dopita et al. (2016) is shown in purple circles. A sample of star-forming galaxies from MaNGA are shown in black squares (Belfiore et al., 2017). The Pilyugin, Vílchez & Thuan (2010), Berg et al. (2012), Izotov, Thuan & Guseva (2012), and James et al. (2015) measurements are for individual systems, while the Dopita et al. (2016) and Belfiore et al. (2017) data represent a population-averaged trend. Error bars are omitted for visual clarity.

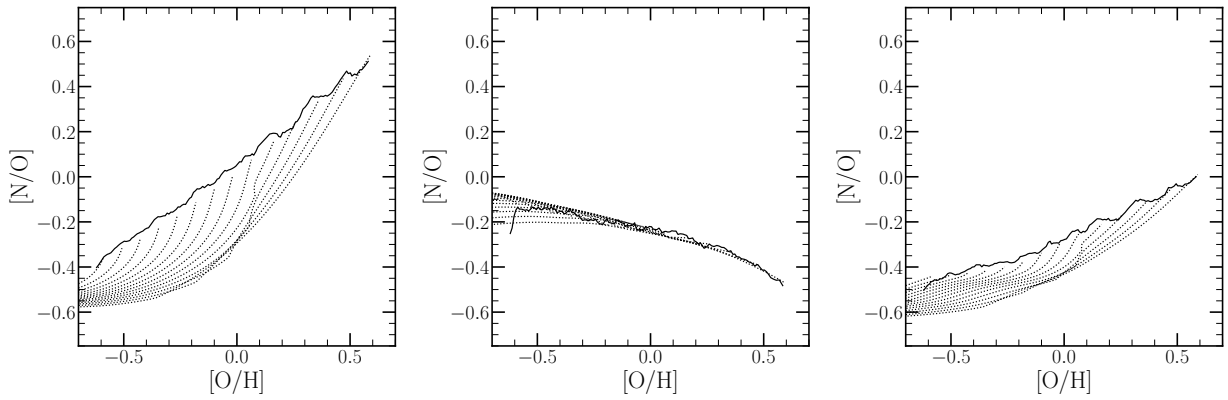

Figure 9: The present-day gas-phase [N/O] relation as a function of [O/H] in the fiducial model for $R_{\rm gal} \geq 2$ kpc (solid), shown alongside the gas-phase evolutionary tracks (i.e. parameterized by time) for $R_{\rm gal} = 2$, 3, 4, ... , 13, 14, and 15 kpc rings. Each panel shows a different set of AGB star yields: Cristallo et al. (2011) on the left, Karakas (2010) in the middle, and Ventura et al. (2013) on the right.

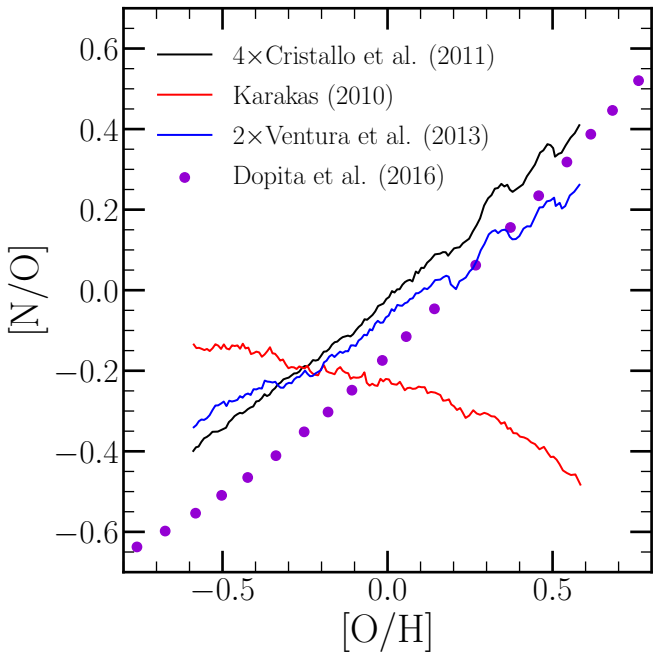

Figure 10: The present-day gas-phase [N/O]-[O/H] relation in the fiducial model for $R_{\rm gal} \geq 2$ kpc assuming three different AGB star yield prescriptions for N: the Cristallo et al. (2011, 2015) sample amplified by a factor of 4 (black), the Karakas (2010) sample (un-amplified, red), and the Ventura et al. (2013) sample amplified by a factor of 2 (blue). For reference, the Dopita et al. (2016) calibration is plotted in purple points.

Can we distinguish between the different AGB star yield sets? In Fig. 10, we compare the predicted present-day gas-phase [N/O]-[O/H] relation in the inside-out SFH model ran with a few different prescriptions for the AGB star yield. Both the Cristallo et al. (2011, 2015) and Ventura et al. (2013) sets can reproduce the observed trend within the scatter to a reasonable accuracy, though a multiplicative prefactor is required to do so, suggesting that these models under-predict nitrogen production. The Karakas (2010) model, however, fails to reproduce the trend, instead predicting an [N/O]-[O/H] relation which is montonically *decreasing*. There is no multiplicative prefactor which can be added to this yield set to reproduce the observed relation.

Bibliography

Asplund M., Grevesse N., Sauval A. J., Scott P., 2009, ARA&A, 47, 481

Belfiore F., et al., 2017, MNRAS, 469, 151

Berg D. A., et al., 2012, ApJ, 754, 98

Cristallo S., et al., 2011, ApJS, 197, 17

Cristallo S., Straniero O., Piersanti L., Gobrecht D., 2015, ApJS, 219, 40

Dopita M. A., Kewley L. J., Sutherland R. S., Nicholls D. C., 2016, Ap&SS, 361, 61

Henry R. B. C., Edmunds M. G., Köppen J., 2000, ApJ, 541, 660

Izotov Y. I., Thuan T. X., Guseva N. G., 2012, A&A, 546, A122

James B. L., Koposov S., Stark D. P., Belokurov V., Pettini M., Olszewski E. W., 2015, MNRAS, 448, 2687

Johnson J. W., Weinberg D. H., 2020, MNRAS, 498, 1364

Johnson J. W., et al., 2021, arXiv e-prints, p. arXiv:2103.09838

Karakas A. I., 2010, MNRAS, 403, 1413

Kroupa P., 2001, MNRAS, 322, 231

Limongi M., Chieffi A., 2018, ApJS, 237, 13

Nomoto K., Kobayashi C., Tominaga N., 2013, ARA&A, 51, 457

Pilyugin L. S., Vílchez J. M., Thuan T. X., 2010, ApJ, 720, 1738

Sukhbold T., Ertl T., Woosley S. E., Brown J. M., Janka H. T., 2016, ApJ, 821, 38

Ventura P., Di Criscienzo M., Carini R., D'Antona F., 2013, MNRAS, 431, 3642

Vincenzo F., Belfiore F., Maiolino R., Matteucci F., Ventura P., 2016, MNRAS, 458, 3466

Weinberg D. H., Andrews B. H., Freudenburg J., 2017, ApJ, 837, 183

Woosley S. E., Weaver T. A., 1995, ApJS, 101, 181